

Studies on the Molecular & Electronic Structure, Stability, Thermochemical and Spectroscopic Properties of Ru(II)-Porphyrin Derivatives – A Theoretical Insight

Dileep D¹, Rajesh R¹, Sivasankar B N¹ and Krishnamoorthy Bellie Sundaram^{2*}

1 Department of Chemistry, Government Arts College, Udthagamandalam, The Nilgiris, Tamil Nadu, India, 643 002;

2 Department of Chemistry (SF), PSG College of Arts and Science, Coimbatore – 641014, Tamil Nadu, India.

Abstract: Ruthenium-porphyrin compounds are interesting for research due to the different possible oxidation states for ruthenium which lead to diverse structural preferences with wider applications. The Ruthenation of porphyrin and substitutions in the Ru(IV) versus Ru(II) porphyrins with different R groups is an interesting area of research. The stability, molecular structural features and spectroscopic properties of the different Ruthenium(II)-porphyrin compounds of the type Ru^{II}P, where, P = porphyrin (1); Octamethylporphyrin (2); Octaethylporphyrin (3); Octa-n-propyl-porphyrin (4); Octa-isopropyl-porphyrin (5); Octa-n-butyl-porphyrin (6) and Octa-tert-butyl-porphyrin (7) are studied using density functional theory (DFT) methods at BP86/Def2-TZVP level. Computational studies predict the stable nature of these compounds and the obtained geometries are minima in their potential energy surface. The localization of the free electrons of these triplet state compounds in the dz² and dxy orbitals are also revealed.

Key words: Ru(II)-porphyrin; DFT; Alkyl substitution; Molecular Orbital Analysis;

Introduction:

Ru(II)-porphyrins typically feature a central ruthenium ion coordinated to a porphyrin macrocycle. The porphyrin acts as a dianionic tetradentate ligand, stabilizing the Ru(II) oxidation state. These complexes often include axial ligands, such as carbon monoxide (CO), pyridine, or phosphines, which influence their electronic and structural properties.[1] The ruthenium can be coordinated to one or two axial ligands in addition to the porphyrin, such as phosphines (PPh₃), carbonyl (CO), or pyridines, leading to either five-coordinate (monodentate axial ligand) or six-coordinate (bis-axial ligand) complexes. The Ru(II) ion in these complexes exhibits low-spin d⁶ electronic configuration, contributing to their stability and unique optical properties. Ru(II)-porphyrins are versatile in ligand substitution reactions. For example, CO ligands can be replaced by stronger σ -donor or π -acceptor ligands under mild conditions. Photochemical reactions can also modify these complexes, such as replacing CO with other ligands in weakly coordinating solvents. Strong π -back donation from Ru(II) to ligands like CO results in characteristic low-frequency CO stretching vibrations, which are useful for spectroscopic studies. The metalation of porphyrins is typically achieved by reacting the free-base porphyrin with a metal salt (or complex) in an organic solvent like chloroform, toluene, or DMF. This process tends to be slow, with a high activation barrier primarily due to the distortion required in the relatively rigid porphyrin ring to form the first bond between a pyrrole nitrogen and the metal. This initial bond formation is believed to be the rate-limiting step. [1] Ruthenium porphyrins were synthesized as low-spin, air-stable biomimetic models of Iron(II) porphyrins, which are more stable and inert, especially when interacting with oxygen, compared to their iron counterparts. Ruthenium porphyrins have also been explored as catalysts, particularly for oxidation reactions, as well as for their potential use in sensing applications. Ru(II)-porphyrins are used in catalytic processes, including oxidation and hydrogenation reactions, due to their ability to stabilize reactive intermediates. Their strong

axial bonding with pyridyl ligands makes them ideal for constructing supramolecular assemblies. These complexes are explored for their interactions with biomolecules, such as DNA, and their potential as imaging agents or therapeutic tools. Recent studies focus on the development of Ru(II)-porphyrins for anticancer applications, leveraging their selective reactivity and cellular uptake. Their photophysical properties are being harnessed for applications in light-harvesting systems and photodynamic therapy. Researchers have synthesized and investigated ruthenium(II) porphyrin dimers and tetramers with different axial ligands for their potential applications in catalysis and energy transfer. [2] Solutions of bis(triphenylphosphine)(tetraphenylporphyrinato)-ruthenium(II) had been used for the decarbonylation of aromatic and aliphatic aldehydes. [3] The recent developing and advanced techniques like quantum chemical calculations are crucial in analyzing the potential of molecules.[4-8] Computational studies have been proved to be a successful tool in many cases including metal complexes of structural importance which require more insight. [9-15]. Ruthenium(II) complexes of meso-tetraphenylporphyrin and octaethylporphyrin have already been studied for the reversible binding of dioxygen to the metal centre in order to mimic the heme function. The activation of porphyrins towards O₂ or CO can be done using the suitable labile axial ligands for example acetonitrile.

Here we have studied the electronic, geometric structural features and spectroscopic properties of the different Ruthenium(II)-porphyrin compounds of the type Ru^{II}P, where, P = porphyrin (1); Octamethylporphyrin (2); Octaethylporphyrin (3); Octa-n-propyl-porphyrin (4); Octa-isopropyl-porphyrin (5); Octa-n-butyl-porphyrin (6) and Octa-tert-butyl-porphyrin (7). Ruthenium-porphyrin compounds are very interesting for research due to the various possible oxidation states which lead to diverse structural preferences with wider applications. The Ruthenation of porphyrin and substitutions in the Ru(IV) versus Ru(II) porphyrins with different R groups is an interesting area of research. Computational chemistry tools like DFT

methods can aid to study and model compounds with experimental handling difficulties. Here we have studied the viability of the different ruthenium(II)-porphyrin compounds with substitutions at the porphyrin ring.

Computational Details

Computational chemistry has been used to characterize new compounds with metals and already reported compounds lacking complete structural characterization [16]. All the calculations at the Density Functional Theory level were carried out using the ORCA program developed by F. Neese and co-workers. [17]. The Vosko-Wilk-Nusair parameterization was used for the local density approximation (LDA) with gradient corrections for exchange (Becke88) and correlation (Perdew86) [18-21]. TZVP (triple zeta valence with polarization function) basis set was used for all the molecules. In all the calculations, TightSCF convergence criteria were used [22]. Optimized geometries were checked by the following frequency calculations in order to check that the obtained geometry is the minima minimum [23, 24]. Further, the DFT-optimized geometries were used to calculate the NMR parameters like shielding constants, chemical shifts etc., with the help of the EPRNMR module available in the ORCA software [25]. Tetramethylsilane (TMS) was used as a reference for the calculation of ^1H and ^{13}C NMR chemical shift values [26, 27]. The reactivity descriptors like chemical potential (μ), hardness (η), softness (S), and electrophilicity (ω) are computed using the HOMO and LUMO energies with the following expressions. Chemical potential (μ) = $E_{\text{LUMO}} + E_{\text{HOMO}}/2$; Hardness (η) = $E_{\text{LUMO}} - E_{\text{HOMO}}/2$; Softness (S) = $1/\eta$; Electrophilicity (ω) = $\mu^2/2\eta$; The DFT computed global reactivity descriptors are already proved to be successful in predicting the reactivities of the compounds studied and being used to describe the reactive sites of these important clusters [28]

Results and Discussion

Geometry

The DFT (BP86/TZVP) optimized molecular structures result as minima in the potential energy surface, and the bond parameters are in good agreement with those of a similar compound with tetraphenylporphyrinato derivative. The DFT (BP86/TZVP) optimized molecular structures result as minima in the potential energy surface, and the bond parameters are in good agreement with those of a similar compound with tetraphenylporphyrinato derivative.

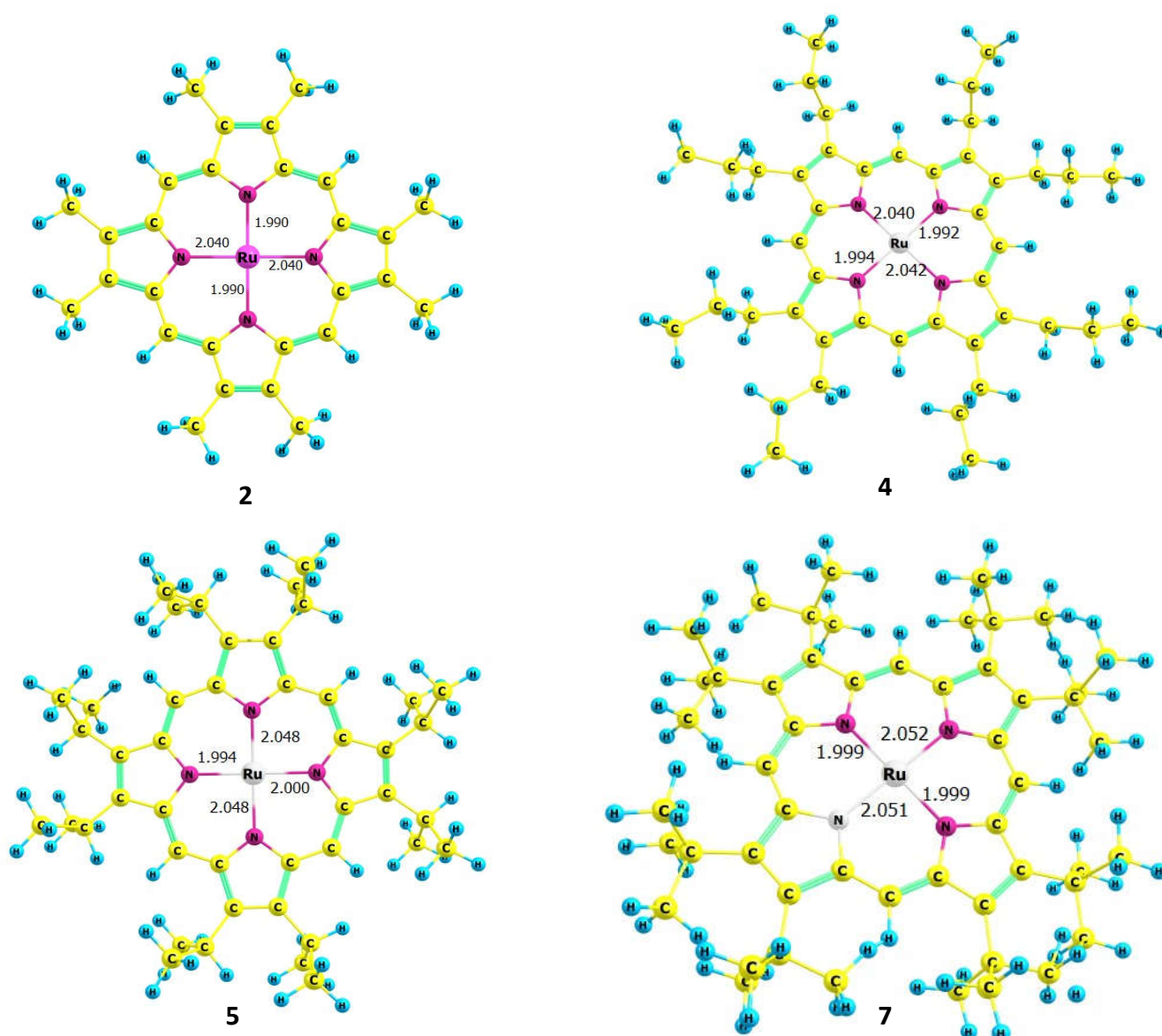


Fig-1; DFT (BP86/Def2-TZVP) optimized geometries of compounds 1-7. $Ru^{II}P$, where, P= Octamethylporphyrin (2); Octa-n-propyl-porphyrin (4); Octa-isopropyl-porphyrin (5); and Octa-tert-butyl-porphyrin (7)

In all these cases the ruthenium atom is in its triplet state. Optimization carried out by considering these compounds as in singlet state are not fruitful in leading to minimum energy structure. The triplet state is playing an important role in the stabilities of these Ru(II)-porphyrinato compounds 2-7 studied in this work. The average Ru-N bond lengths are ranging from 1.990 Å – 2.052 Å which are more close to the Ru-N bond reported already with the crystal structure. [29]

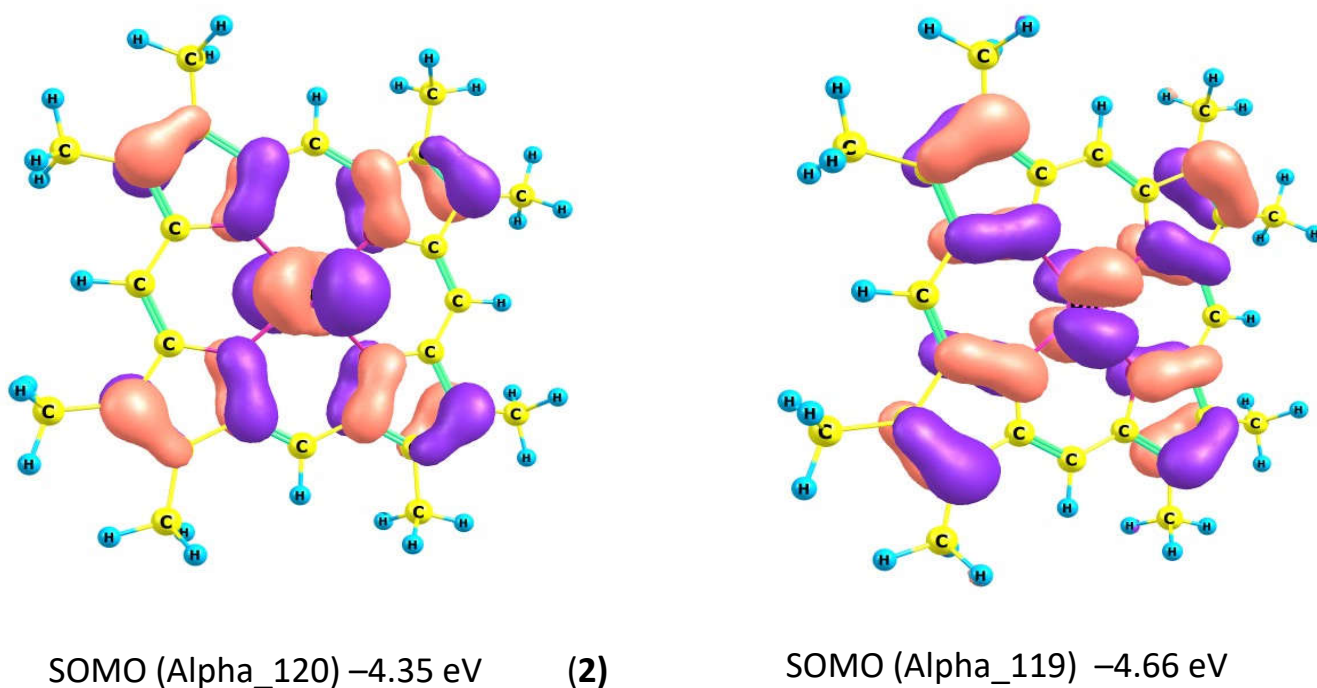


Fig-2; The frontier molecular orbitals (FMO) of the compound (2) obtained from the DFT (BP86/Def2-TZVP) optimized geometry. Ru^{II}P, where, P= Octamethylporphyrin (2);

Electronic Structure

DFT(BP86/Def2-TZVP) optimized geometry of the octamethylporphyrinato ruthenium(II) compound in its triplet state obtained as a minima and the two unpaired electrons are present in the FMOs as shown in the Fig.2. The frontier molecular orbital energies, and the $E_{\text{LUMO-HOMO}}$ computed by the DFT method at BP86/Def2-TZVP level confirm the possible

existence and the stability of the modeled Ru(II)porphyrin compounds 1-7 in their triplet state. The singly occupied molecular orbitals Alpha_120 and Alpha_119 are mainly from the single electrons. The electron is residing in its dz^2 orbital in the alpha_120 and another free electron is residing at the dxy orbital in the alpha_119. Still there are electron densities are around the pyrrole rings.

The density functional theory computed frontier molecular orbitals of metal-porphyrin compounds have already been effectively utilized for predicting the electrical conductance and thermoelectric power of beta-substituted metal-porphyrin molecular junctions.[30] The reactions involving carbene transfer and hydrogen atom transfer in ruthenium porphyrin complexes containing quinoid carbene groups have been documented and demonstrated to function as successful catalysts.[31]

Bond Order Analysis

The Mayer bond analysis (MBA) describes the number of bonds and the various types of bonds present between two atoms, as shown in Table 1. The Sn-N bond orders are ranging from 0.63 to 0.65. The strong Sn-N bonding interaction is exhibited by compound (4) with a bond order value of 0.65. Compounds (2) (5) and (7) also show considerable Sn-N bonding with bond order 0.63. ;

Table 1. DFT computed Mayer bond order (MBO) analysis of the compounds 2-7. Ru^{II}P, where, P= Octamethylporphyrin (2); Octaethylporphyrin (3); Octa-n-propyl-porphyrin (4); Octa-isopropyl-porphyrin (5); Octa-n-butyl-porphyrin (6) and Octa-tert-butyl-porphyrin (7)

S.No	Ru –N1	Ru– N2	Ru– N3	Ru– N4
2	0.6328	0.6322	0.6324	0.6329
3	0.6318	0.6330	0.6323	0.6391

4	0.6488	0.6480	0.6343	0.6491
5	0.6382	0.6380	0.6348	0.6384
6	0.6362	0.6340	0.6328	0.6381
7	0.6361	0.6336	0.6345	0.6368

Bond order analysis confirms the strong bonding interactions between Ru-N atoms. Bonding interactions are easily measured by means of computing the bond orders for each bond. The higher the value stronger the bonding interaction and the existence of multiple bonds can also be ascertained through the bond order computations. Though the synthesis and structural elucidation of some bis(tertiary phosphine) like Ru(octaethylporphyrin)(PPh₃), Ru(meso-tetraphenylporphyrin)(PPh₃), Ru(*meso*-tetraphenylporphyrin){P(*p*-CH₃-C₆H₄)₃}₂, Ru(octaethylporphyrin){P(*p*-CH₃-C₆H₄)₃}₂, Ru(meso-tetraphenylporphyrin)(PBu₃)₂ and carbonyl(tertiary phosphine) like Ru(*meso*-tetraphenylporphyrin)(CO)PPh₃ of Ru(II) are already reported [32] ruthenium(II)-porphyrin chemistry is an active field of research for catalysis, material applications and biological applications.

Conclusions

The Ru(II)-porphyrin complexes are important compounds due to their diverse structural features and wider applications. The electronic, geometric structural features and spectroscopic properties of the different Ruthenium(II)-porphyrin compounds of the type Ru^{II}P, where, P = porphyrin (1); Octamethylporphyrin (2); Octaethylporphyrin (3); Octa-*n*-propyl-porphyrin (4); Octa-*isopropyl*-porphyrin (5); Octa-*n*-butyl-porphyrin (6) and Octa-*tert*-butyl-porphyrin (7) are studied using DFT (BP86/Def2-TZVP) computations. From the theoretical investigation, the following conclusions are made.

The DFT (BP86/TZVP) optimized molecular structures result as minima in the potential energy surface, and the bond parameters are in good agreement with those of a similar compound with tetraphenylporphyrinato derivative. In all these cases the ruthenium atom is in its triplet state.

The frontier molecular orbital energies, and the $E_{\text{LUMO-HOMO}}$ computed by the DFT method at BP86/Def2-TZVP level confirm the possible existence and the stability of the modeled Ru(II)porphyrin compounds 1-7.

The DFT computed metrical parameters of these ruthenium(II)-porphyrins are very close to those of the experimental values of the similar compounds. The average Ru-N bond lengths are ranging from 1.990 Å – 2.052 Å which are more close to the Ru-N bond reported already with the crystal structure.

Bonding analysis of the frontier molecular orbitals suggests that the singly occupied molecular orbitals are mainly from the single electrons. The electron is residing in its d_{z^2} orbital in the and another free electron is residing at the d_{xy} orbital in the case octamethylporphyrinoruthenium(II) **2**.

The Mayer bond analysis (MBA) predicts that the strong Ru-N bonding interaction is exhibited by compound (4) with a bond order value of 0.65 and the remaining compounds also show considerable Ru-N bonding interaction with the bond order value of about 0.63.

DFT computations has proved to be successful in predicting the stability and structural features of the ruthenium-porphyrins and helpful in designing the new molecules.

References

1. Massoudipour, M., Pandey, K K, Preparation and characterization of ruthenium(II) porphyrins, *Inorganica Chimica Acta*, 1989, 160 (1), 115-118.
[https://doi.org/10.1016/S0020-1693\(00\)85410-9](https://doi.org/10.1016/S0020-1693(00)85410-9)
2. He, L., Chan, P. W. H , Tsui, W-M, Yu, W-Y, Che, C-M., Ruthenium(II) Porphyrin Catalyzed Amidation of Aromatic Heterocycles, *Org. Lett.* 2004, 6, 14, 2405–2408.
<https://doi.org/10.1021/ol049232j>
3. Domazetis, G., Tarpey, B., Dolphin, D. and James, B. R., Catalytic decarbonylation of aldehydes using ruthenium(II) porphyrin systems, *J Chem. Soc., Chem. Commun.*, 1980, 939-940 <https://doi.org/10.1039/C39800000939>
4. Wang, N.; Liu, H.; Zhao, J.; Cui, Y.; Xu, Z.; Ye, Y.; Kiguchi, M.; Murakoshi, K. Theoretical investigation on the electron transport path through the porphyrin molecules and chemisorption of CO. *J. Phys. Chem.* **2009**, *113* (17), 7416– 7423, DOI: 10.1021/jp900335p;
5. Noori, M.; Sadeghi, H.; Lambert, C. J. High-performance thermoelectricity in edge-over-edge zinc-porphyrin molecular wires. *Nanoscale* **2017**, *9* (16), 5299– 5304, DOI: 10.1039/C6NR09598D
6. Cook, L. P.; Brewer, G.; Wong-Ng, W. Structural aspects of porphyrins for functional materials applications. *Crystals* **2017**, *7* (7), 223 DOI: 10.3390/cryst7070223
7. Li, Y.; Yao, J.; Zhong, S.; Zou, Z. Theoretical investigations on the orientational dependence of electron transport through porphyrin molecular wire. *Curr. Appl. Phys.* **2011**, *11* (6), 1349– 1353, DOI: 10.1016/j.cap.2011.04.001
8. Karlström, O.; Linke, H.; Karlström, G.; Wacker, A. Increasing thermoelectric performance using coherent transport. *Phys. Rev. B* **2011**, *84* (11), 113415 DOI: 10.1103/PhysRevB.84.113415

9. Nagalakshmi V, and Nandhini R, Brindha V, Krishnamoorthy B. S and Balasubramani K, *J. Organomet. Chem.*, **2020**, 912, 121175. DOI: [10.1016/j.jorganchem.2020.121175](https://doi.org/10.1016/j.jorganchem.2020.121175);
10. Krishnamoorthy, B. S. Kahlal, S., Ghosh S., and J-F. Halet, Electronic, geometrical, and thermochemical studies on group-14 element-diruthenaborane cluster compounds: a theoretical investigation, *Theoretical Chemistry Accounts*, **2013**, 132, 1356, <https://doi.org/10.1007/s00214-013-1356-6>
11. Bharathi K, Beerma L, Santhi C, Krishnamoorthy B. S., and Halet, J-F, Structural, electronic and magnetic properties of some early vs late transition dimetallaborane clusters – A theoretical investigation, *J. Organomet. Chem.*, **2015**, 792, 220—228, <https://doi.org/10.1016/j.jorganchem.2015.05.057>.
12. S. Gomathi, K. Kavitha, N. Savitha, A. Mohana, V. Brindha, B. S. Krishnamoorthy , Molecular Structure, Reactivity and Spectroscopic Properties of Hallucinogens Psilocybin, Mescaline and their Derivatives – A Computational Study, *Letters in Applied NanoBioScience*, **2023**, 12, 105, <https://doi.org/10.33263/LIANBS124.105>
13. Nandhini R, Krishnamoorthy B S, Venkatachalam G, Binuclear half-sandwich ruthenium(II) Schiff base complexes: Synthesis, characterization, DFT study and catalytic activity for the reduction of nitroarenes, *J. Organomet. Chem.*, **2019**, 903, 120984;
14. Brindha V and Krishnamoorthy B S, Isomer Preferences and Structural Studies on Cobaltaboranes – A Theoretical Investigation, [Biointerface Research in Applied Chemistry](https://doi.org/10.33263/LIANBS124.105), **2024**, 14, 73. [BRIAC143.073.pdf \(biointerfaceresearch.com\)](https://doi.org/10.33263/LIANBS124.105).
15. Arumugam N., Soliman S.M., Viswanathan V., Almansour A.I., Kumar R.S., Mahalingam S.M., Krishnamoorthy B.S., Dege N., Karuppiah P., Perumal K., Environmentally-friendly synthesis, structural determination and antimicrobial activity of new class of spiropyrrolidine embedded with indenoquinoxaline and chromanone

- heterocyclic units, *J. of Mol. Struct.*, **2023**, 1293, 136189.
<https://doi.org/10.1016/j.molstruc.2023.136189>
16. Patel, T.R.; Ganguly, B. Exploring the metal-free catalytic reduction of CO₂ to methanol with saturated adamantane scaffolds of phosphine-borane frustrated Lewis pair: A DFT study. *J. Mol. Graph. Model.* 2022, 113, 108150, <https://doi.org/10.1016/j.jmglm.2022.108150>
17. Neese, F. Software update: The ORCA program system—Version 5.0. *WIREs Comput. Mol. Sci.* 2022, 12, e1606, <https://doi.org/10.1002/wcms.1606>.
18. Vosko, S.H.; Wilk, L.; Nusair, M. Accurate spin-dependent electron liquid correlation energies for local spin density calculations: a critical analysis. *Can. J. Phys.* 1980, 58, 1200-1211, <http://doi.org/10.1139/p80-159>.
19. Becke, A.D. Density functional calculations of molecular bond energies. *J. Chem. Phys.* 1986, 84, 4524-4529, <https://doi.org/10.1063/1.450025>.
20. Becke, A.D. Density-functional exchange-energy approximation with correct asymptotic behavior. *Phys. Rev. A* 1988, 38, 3098, <https://doi.org/10.1103/PhysRevA.38.3098>.
21. Perdew, J.P. Density-functional approximation for the correlation energy of the inhomogeneous electron gas. *Phys. Rev. B*, 1986, 33, 8822, <https://doi.org/10.1103/PhysRevB.33.8822>.
22. Weigend, F.; Ahlrichs, R. Balanced basis sets of split valence, triple zeta valence and quadruple zeta valence quality for H to Rn: Design and assessment of accuracy. *Phys. Chem. Chem. Phys.* 2005, 7, 3297-3305, <https://doi.org/10.1039/b508541a>.
23. Reveles, J.U.; Köster, A.M. Geometry optimization in density functional methods. *J. Comput. Chem.* 2004, 25, 1109–1116, <https://doi.org/10.1002/jcc.20034>.

24. Schlegel, H.B. Geometry optimization. WIREs Comput. Mol. Sci. 2011, 1, 790–809, <https://doi.org/10.1002/wcms.34>.
25. Mareš, J., Vaara, J. Ab initio paramagnetic NMR shifts via point-dipole approximation in a large magnetic-anisotropy Co(II) complex. Phys. Chem. Chem. Phys. 2018, 20, 22547-22555, <https://doi.org/10.1039/C8CP04123G>.
26. Becker, E.D. Chapter 4 - Chemical Shifts. In High Resolution NMR (Third Edition), Academic Press, 2000, 83-117, <https://doi.org/10.1016/B978-012084662-7/50048-X>.
27. Guzman, A.L.; Hoye, T.R. TMS is Superior to Residual CHCl₃ for Use as the Internal Reference for Routine ¹H NMR Spectra Recorded in CDCl₃. J. Org. Chem. 2022, 87, 905–909, <https://doi.org/10.1021/acs.joc.1c02590>.
28. Oller, J., Pérez, P., Ayers, P.W., Vöhringer-Martinez, E., Global and local reactivity descriptors based on quadratic and linear energy models for α,β -unsaturated organic compounds. Int. J. Quantum. Chem. 2018, 118, e25706, <https://doi.org/10.1002/qua.25706>.
29. Funatsu, K., Kimura, A., Imamura, T., Ichimura, A. and Sasaki, Y., Perpendicularly Arranged Ruthenium Porphyrin Dimers and Trimers, Inorg. Chem. 1997, 36, 8, 1625–1635. <https://doi.org/10.1021/ic961154b>
30. Li Y., Chan P. W. H., Zhu N-Y., Che C. –M. and Kwong H-L, Ruthenium(II) porphyrin catalyzed imine aziridination and crystal structures of (*meso-tetrakis*-(pentafluorophenyl)porphyrinato)ruthenium(II) complexes containing PhN=CH(*p*-ClPh), CPh₂, and pyridine ligands, *Organometallics*, **2004**, 23, 54-66. <https://doi.org/10.1021/om034128b>
31. Wang H-X, Wan Q, Wu K, Low K-H, Yang C, Zhou C-Y, Huang J-S and Che C-M, Ruthenium(II) Porphyrin Quinoid Carbene Complexes: Synthesis, Crystal Structure,

and Reactivity toward Carbene Transfer and Hydrogen Atom Transfer Reactions, *J. Am. Chem. Soc.* **2019**, 141, 22, 9027–9046. <https://doi.org/10.1021/jacs.9b03357>

- 32.** Sara A., David D., George D., Brian R. J., Tak W. L., Steven J. R., James T., Gregory M. W., Preparation and characterization of some ruthenium(II) porphyrins containing tertiary phosphine axial ligands, including the crystal structure of (octaethylporphinato)bis(triphenylphosphine)ruthenium(II), *Can. J. Chem.*, 1984, 62, 755-762. <https://www.tesble.com/10.1139/v84-127>